25th ABCM International Congress of Mechanical Engineering
October 20-25, 2019, Uberlândia, MG, Brazil

COBEM-2019-1477
FRICTION HIDRO PILLAR PROCESSING APPLIED TO PLATFORM ANCHOR CHAINS WITH USAGE OF PRE AND POST HEATING

Priscila Braia Felippe
Rafael Ariza Gonçalves
Raphael Rezende Pires
Sinésio Domingos Franco
Federal University of Uberlândia, Av. João Naves de Ávila, 2121, Santa Mônica, 38400-902, Uberlândia - MG
pribraia@yahoo.com.br; rafael.ariza@ufu.br; raphaelrpires@yahoo.com.br; sdfranco@ufu.br

Ricardo Reppold Marinho
Marcelo Torres Piza Paes
Petrobras, Centro de Pesquisas e Desenvolvimento Leopoldo Américo M. de Mello, Cidade Universitária, 21941-915, Rio de Janeiro - RJ
reppold@petrobras.com.br; mtpp@petrobras.com.br

Abstract. *Arc welding process is frequently used to repair steel structure defects. But, when applied to the petroleum sector, this technique presents limitations such as: porosity, hydrogen embrittlement and formation of hard microstructures. Friction Hidro Pillar Processing (FHPP) repair technique has great potential for application in the oil and gas industry. It consists in drilling a hole in the cracked region, which will later be filled by friction welding a consumable rod. In this process, the metallurgical bonding is achieved in the solid state and, consequently, lower temperatures are involved being less susceptible to the external environment. Although there was no formation of cracks, the pre and post-heating treatments at temperatures tested initially did not prevent the formation of hard phases such as martensite. This, combined with other unexpected results led to the search of new alternatives for the job, such as the use of higher post-heating temperature, with satisfactory results. The quality control of repairs was done through macrographic and micrographic analysis and hardness profiles.*

Keywords: *Friction hidro pillar processing, pre- and post-heating, repair quality, heat-affected zone*

1. INTRODUCTION

Friction welding occurs by rotation or relative movement of two surfaces, subjected to compression. The heat generated by the frictional forces allows plastic deformation of material from the frictional surfaces, and thus the metallurgical junction of the parts in the solid state (AWS, 1991).

According to Meyer (2003), friction welding being a solid state process, is free from defects associated with solidification such as porosity, segregation and hydrogen adsorption.

The Figure. 1 schematizes the sequence of steps that characterize the process in question. First, one of the parts is rotated (Fig. 1-a). Then, even with this rotational movement, the surfaces are already approximated with the application of compressive force (Fig. 1-b), and then the heat generated causes plastic flow of material to join the two parts (Fig. 1-c). Finally, there may or may not be forging, where an axial force is maintained for a short time, and the welding process is terminated with the formation of the flash (Fig. 1-d).

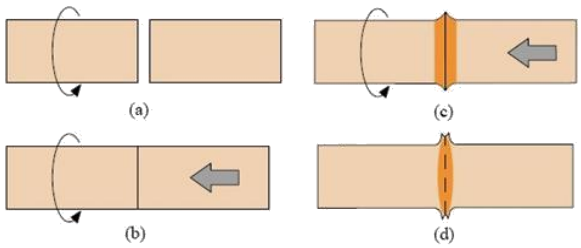

Figure 1: Friction welding. (a) Rotation of one of the parts; (b) Beginning of application of compressive force; (c) Beginning of welded joint; (d) Complete welding (BORGES, 2014).

The friction repair technique is similar to friction welding and basically consists of the following: a non-through hole (cylindrical or conical) is drilled at the location of the crack and then filled with a consumable stud through the application of rotation and axial force on the stud towards the hole.

The friction between the stud and the hole surface generates heat and reduces the flow limit of the material, with the consequent formation of a plastic flow that propagates and completely fills the hole. There is no melting of the base metal (LEBEDEV, 1992). Fig. 2 illustrates the process.

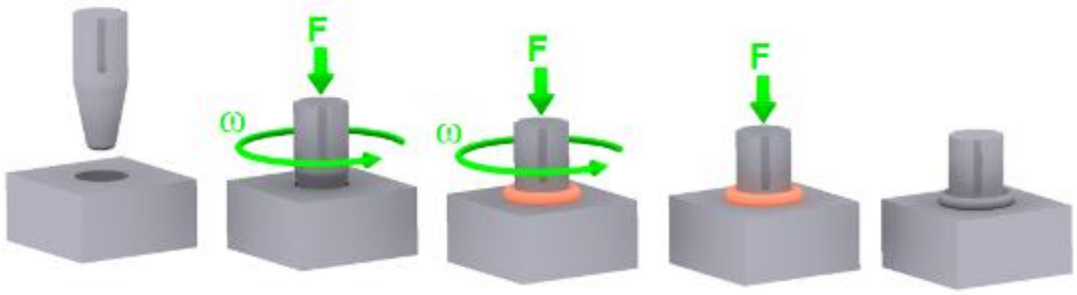

Figure 2: Schematic illustration of the friction repair process (FREITAS, 2014).

The friction repair process has enormous potential, but can generate defects such as formation of hard phases, unfilled regions and cracks, depending on the test conditions. Fig. 3 shows a crack in a friction repair.

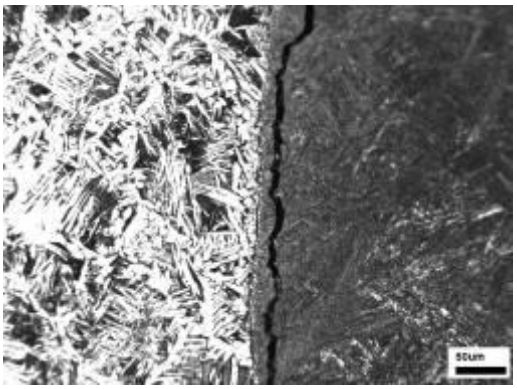

Figure 3. Example of crack generated in a friction repair test.

The objective of the present work is to show the viability of the proposed method to perform repair on oil rig mooring chain links, free of hard phases, cracks and filling defects in general.

2. MATERIALS AND EXPERIMENTALS METHODS

The blocks for carrying out the repair tests were taken from chain links of offshore oil platforms, shown in Fig. 4. The chemical compositions of the repair blocks (chain) and the filler studs are shown in Table 1

Figure 4. Segment of an anchor chain.

Table 1: Chemical composition of chain links (% by weight) (CUNHA, 2013).

Material	Elements													
	C	Si	Mn	P	S	Cu	Al	Cr	Mo	Ni	V	Ti	Nb	Co
Chain Link Block	0,170	0,259	1,229	0,012	----	0,189	0,020	1,763	0,436	1,164	0,019	0,002	0,007	0,018
ABNT 1020 stud	0,20	0,45	0,50	0,03	0,05									

The geometries of the repair blocks and studs are shown in Fig. 5.

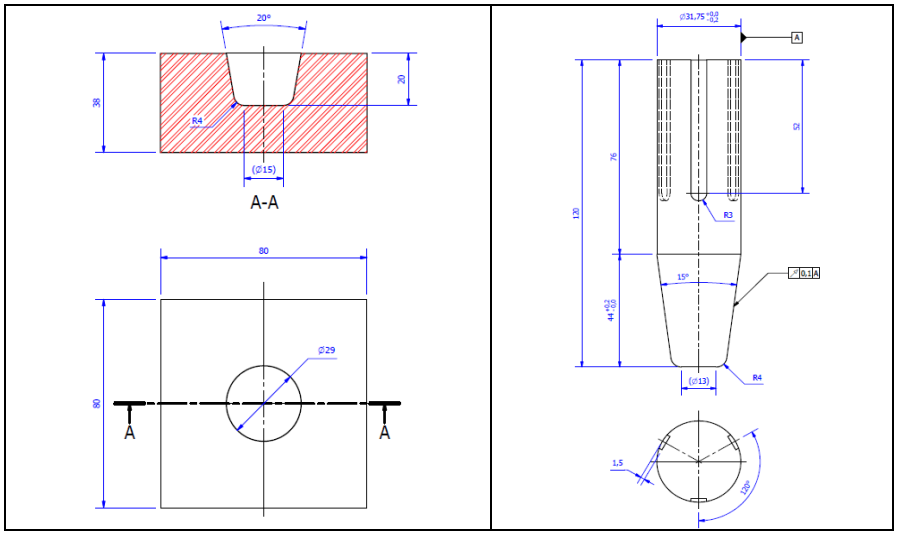

Figure 5. Design of the repair block and the consumable stud.

The friction repair tests were performed using an equipment called Friction Stud Processing Unit III, shown in Fig 6, developed at the UFU by Friction and Wear Technology Laboratory.

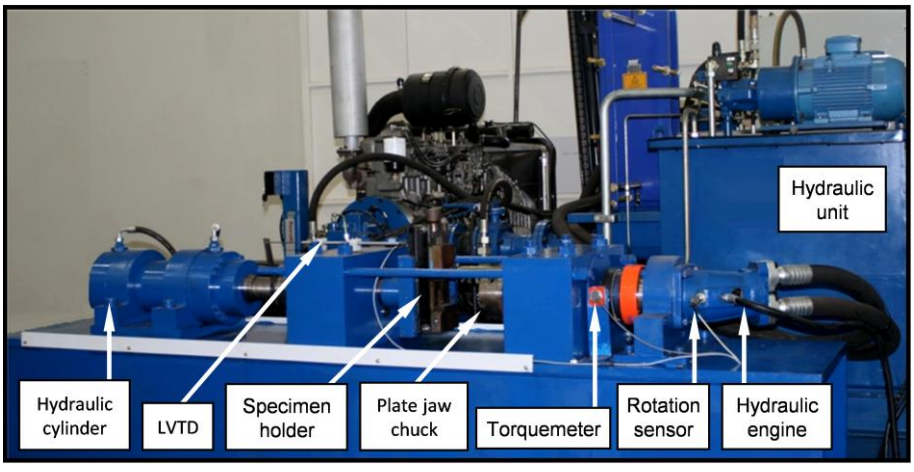

Figure 6: Friction Pin Processing Unit III (PIRES et al., 2014).

In the processing unit, the stud is secured through a plate of nuts and the repair block through a vise. The plate of nuts is driven by a hydraulic motor of axial pistons, allowing rotations of up to 1800 rpm. The vise, on the other hand, is mounted on the end of a hydraulic cylinder capable of applying axial forces up to 500 kN.

The Friction Stud Processing Unit III is equipped with a data acquisition and control system that allows programming the test parameters, controlling the whole process, plotting the variation of the parameters as a function of time, and calculating the required processing power at any moment.

For the preheating tests, an induction heating unit was mounted with a coil that allows the stud to pass through, as shown in Fig. 7.

Figure 7. Repair block fixed on the vise and induction coil that allows the passage of the fill stud through it.

Six trials were performed, as shown in Table 2.

Table 2: Test matrix.

Sample	Force (kN)	Preheating temperature (°C)	Post-heating temperature (°C)
30801	60	-	-
30802	100	-	-
30803	60	300	-
30804	60	300	400
30805	100	300	-
30806	100	300	400

All tests were performed with a rotation of 1700 rpm and burning length of 7 mm. The burn-off length is the distance of the stud offset against the bottom of the block during the test. The burn-off length is completed, the rotation is ceased and the axial force is applied for 10 seconds.

The post heating were performed immediately after the friction hidro pillar processing in an oven for one hour.

After the tests, the next step was to analyze the microstructure of the repaired material to identify aspects of the thermally affected zone and possible defects and failures in the macro and microstructure. For this, the rod/block assembly obtained went through a series of cross sections, preparation for macrographic and micrographic analysis and hardness profiles.

Figure 8 shows a longitudinal section to the stud and the indication of a second cut to reduce the size of the sample.

The micrographs were obtained in the mapped regions, after sanding, polishing and etching with Nital 2 %. In order to perform the micrographs and hardness profiles, they were obtained according to the planning shown in Fig.9, having the origin of the interface rod/block (position 0), made of 1 in 1 mm, with the positions inside the stud negative and positions within the base metal.

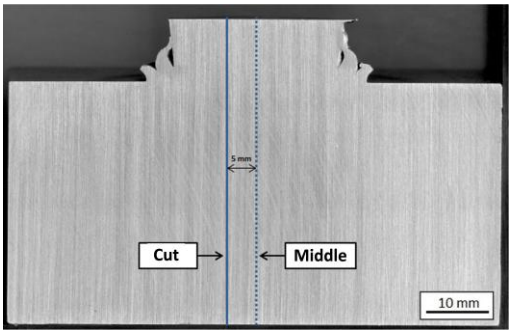

Figure 8: Longitudinal cut of the rod.

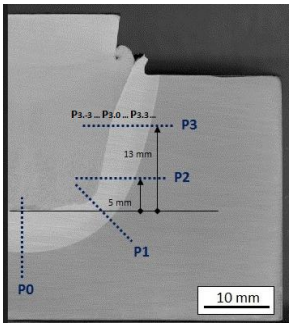

Figure 9. Planning of three hardness profiles and locations to obtain the micrographs.

3. RESULTS AND DISCUSSIONS

The test parameters, force, rotation and burn length, torque and power are recorded in real time by the equipment. Figure 10 shows the records of three tests, where one can see the effect of the axial force and the preheating temperature at the weld duration and consequently the energies provided.

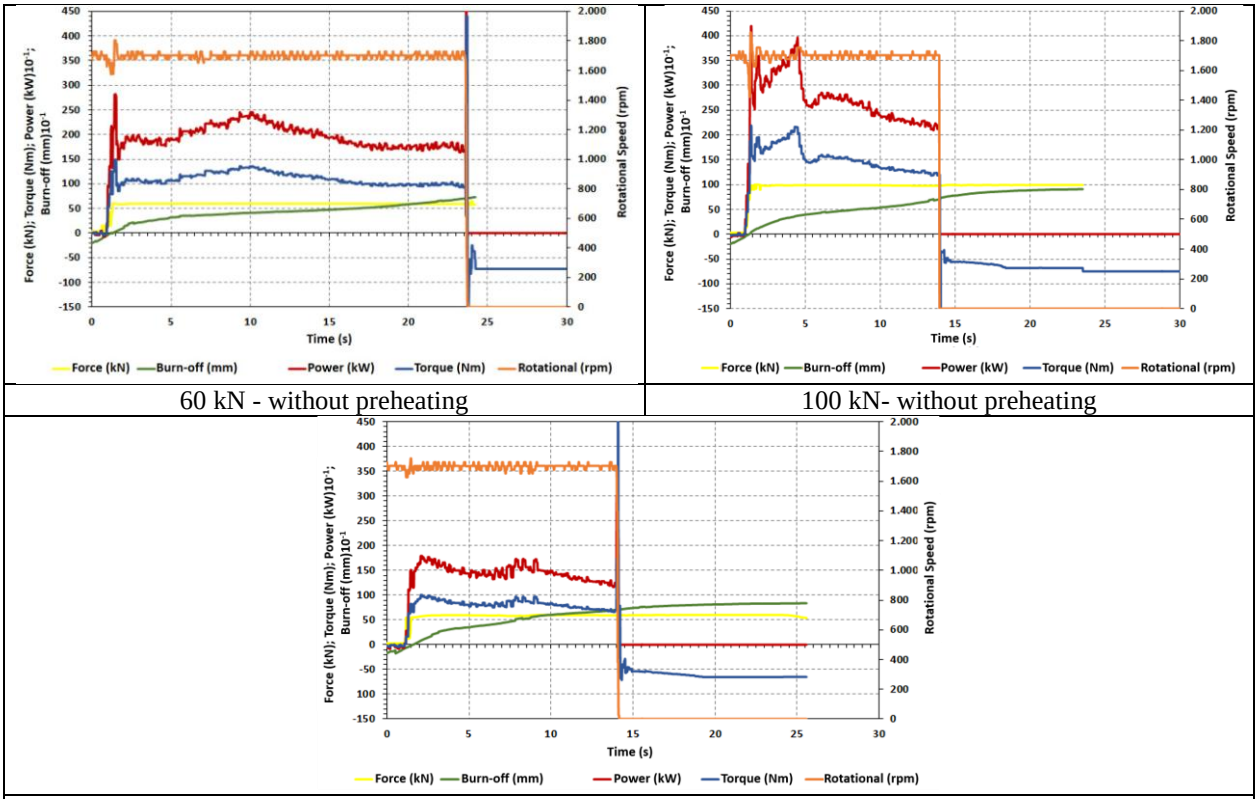

60 kN - without preheating | 100 kN- without preheating

60 kN - preheating 300 °C without post-heating

Figure 10: Data acquired in real time for three of the tests performed.

The graphs show that increasing the axial force and the preheating temperature reduces the time to reach burn-off length and consequently the total welding energy.

Figure 11 shows the macrographs of three block stud assemblies obtained from welding tests with axial force variation, use of preheating and post-heating.

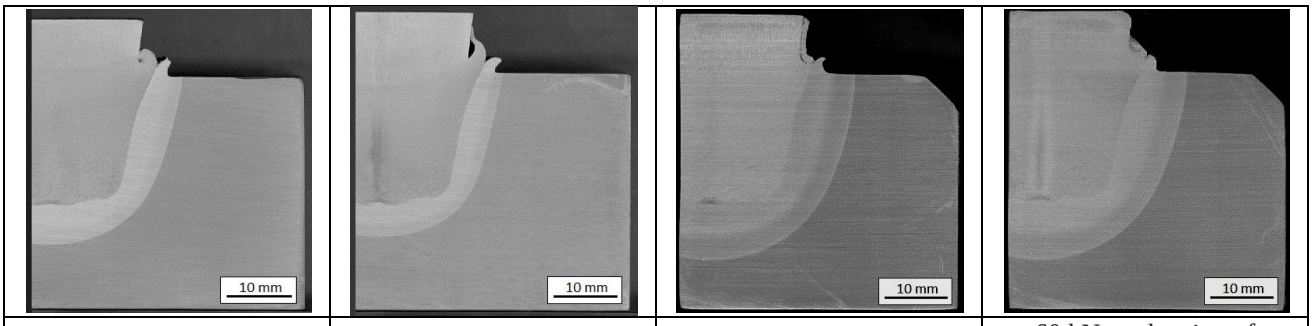

60 kN - without preheating	100 kN- without preheating	60 kN - preheating 300 °C	60 kN, preheating of 300 °C and post-heating of 400 °C

Figure 11. Macrographs obtained.

Figure 12 shows the comparison of the areas of the heat-affected zone of all the samples, measured through the Image J. Software.

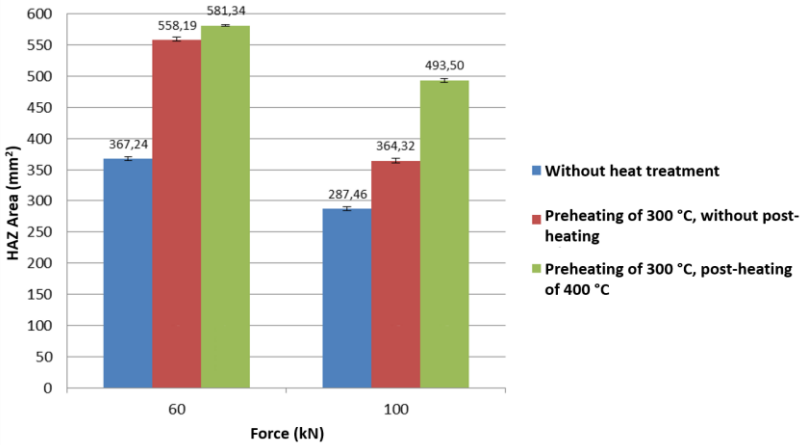

Figure 12: Comparison of the heat-affected zone of the samples tested.

The micrographs obtained in the P2.0 region are shown in Figure 13. The samples were processed with 60 kN without pre- and post-heating (fig. 13a), 100 kN without pre and post-heating (Fig. 13b), 60 kN with preheating of 300 °C, without post heating (Fig. 13c) and 60 kN with preheating of 300 °C and post-heating of 400 °C (Fig. 13d).

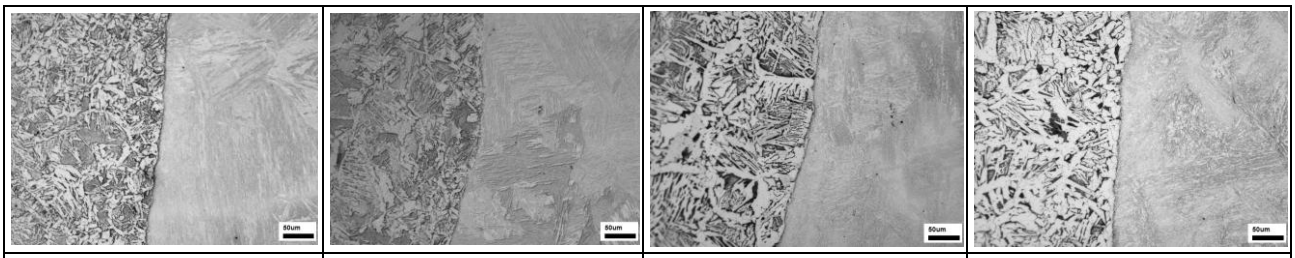

a	b	c	d

Figure 13. Micrographs obtained at the stud/block interface (position 0) in profile P2.0.

Observation of the macrographs and micrographs along the stud/block interfaces reveal that there were no cracks or filling defects.

Vickers hardness tests with 1kgf load and 1 mm spacing were performed, according to the mapping shown in Fig. 12. From the hardness tests, it was possible to construct the hardness graphs of the samples for each profile (Vertical, Diagonal, Bottom Horizontal and Superior Horizontal). The horizontal hardness profiles of 5 mm for axial force tests of 60 kN are shown in Fig.14.

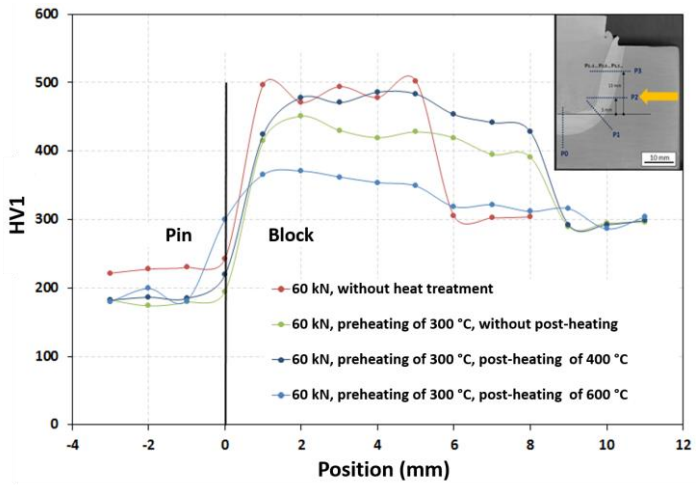

Figure 14. Hardness profiles obtained for samples processed with 60 kN.

The figure shows that there was a reduction of hardness in the thermally affected zone when there was a preheating of 300 °C (green curve) in relation to the hardness obtained from the sample without heating (red curve). The hardness profile of the sample showed that the sample which had undergone the preheating of 300 °C, processed and subsequently heated to 400 °C for one hour, showed an increase of the hardness (dark blue curve). A preheated sample of 300 °C, processed and post-warmed by 600 °C for one hour showed a hardness reduction (light blue curve).

A likely explanation for the increase in hardness caused by tempering at 400 °C is that it would gone through a metallurgical transformation similar to an ausforming heat treatment.

According to Dieter (1976), in thermomechanical ausforming treatment (Fig. 15), the plastic deformation of austenite is performed without transformation into perlite or bainite. Thus, it is necessary to work with a steel in a stable austenite region in its time-temperature-transformation (TTT) diagram. The steel is generally deformed above 50 %, usually by rolling, and then quenched to below the formation temperature of the martensite (Ms) for formation thereof.

The dislocation density of the austempered martensite is very high (10^{13} cm^{-2}) and evenly distributed. The tempering causes the formation of precipitates which contributes to increase the hardness.

For a given alloy, the deformation temperature and the amount of deformation are the main variables.

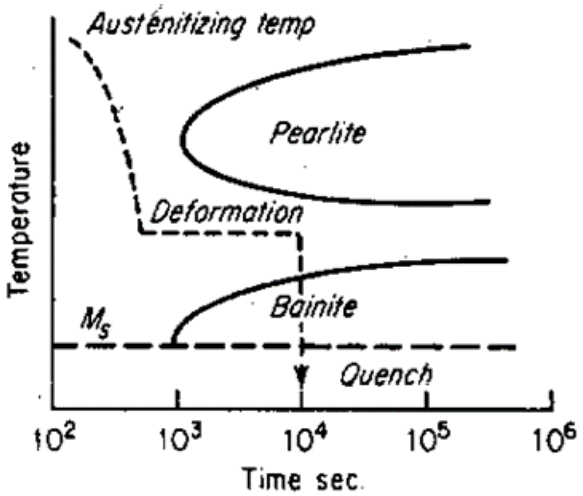

Figure 15. TTT curve showing the process of ausforming (DIETER, 1976).

The steel of the chain links is similar to DIN 17CrNiM06V steel and its TTT curve is shown in Fig. 16.

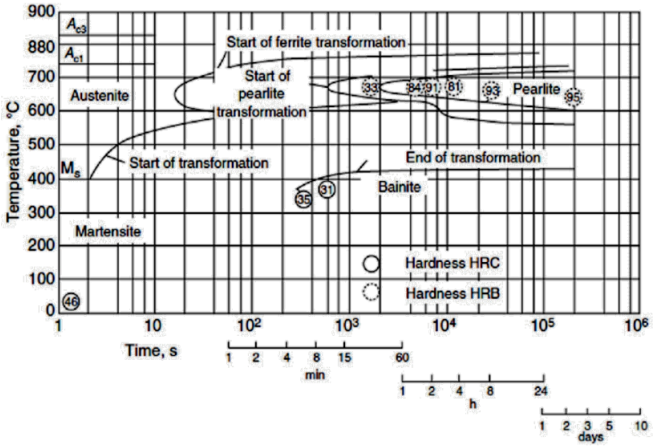

Figure 16: TTT curve of DIN 17CrNiMo6V steel (TOTTEN, 2006).

The processing time was 14 seconds and after that, another 10 seconds of forging was applied. The temperature generated at the interface stud and base metal is about 1100 °C as shown by Gontijo (2012), which guarantees austenitization in its vicinity. Further, the strain rates are very high as shown by the flashes of solid steel and also the deformation at the base stud/metal interface, shown in Fig. 17

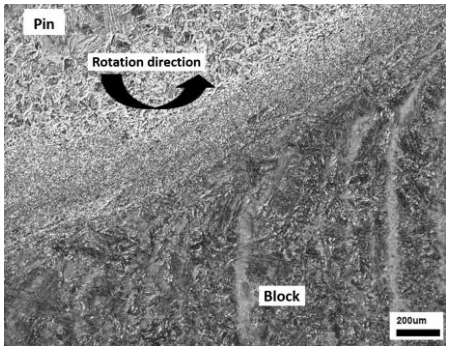

Figure 17. Micrograph of the cross section at position P2 of the sample processed with 60 kN and with preheating of 300 °C. Nital attack 2 %.

Considering that the friction welding is a thermomechanical process, and considering the characteristics of the steel of the anchor chain, it is perfectly possible to have occurred, even to a small extent, the process of ausforming, which would justify the increase of hardness after the tempering of 400 °C.

Hardness profiles similar to those shown in Fig. 14 (60 kN force) were made for the force of 100 kN, shown in Fig. 18.

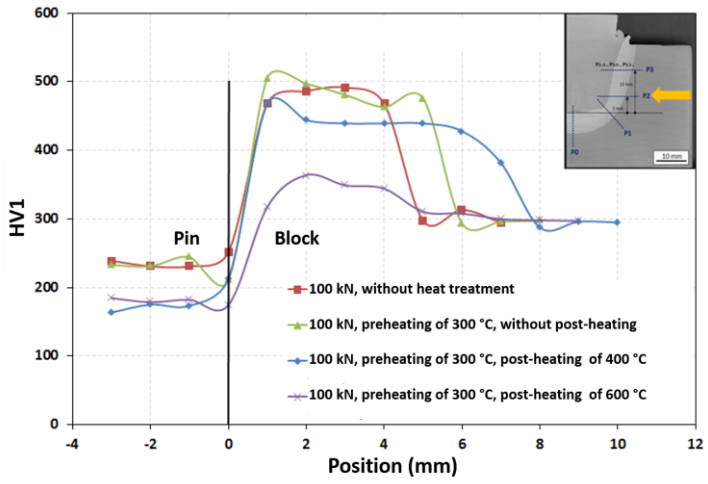

Figure 18. Hardness profiles obtained for samples processed with 100 kN.

In this case it was evident that the preheating of 300 °C (green curve) did not cause hardness lowering compared to the sample without preheating (red curve). The post-heating of 400 °C did not cause increase in hardness but rather a decrease (blue curve), probably because, in this case, due to the shorter processing time, no ausforming occurred.

In order to reduce hardness peaks reached (500 HV), tempering at 600 °C was performed with the hardness profiles shown in Figs. 19 and 20.

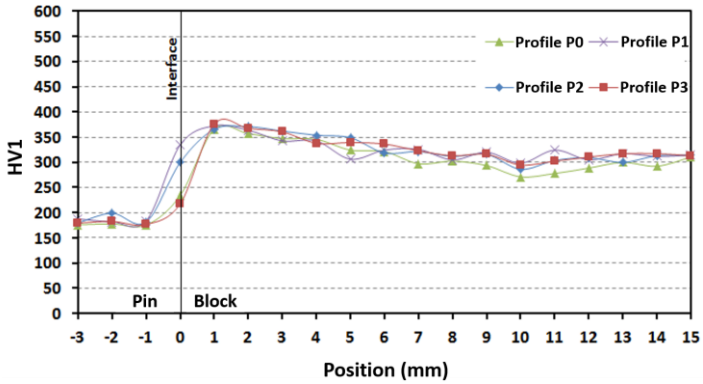

Figure 19: Sample hardness profiles (60 kN, preheating 300 °C and post heating at 600 °C).

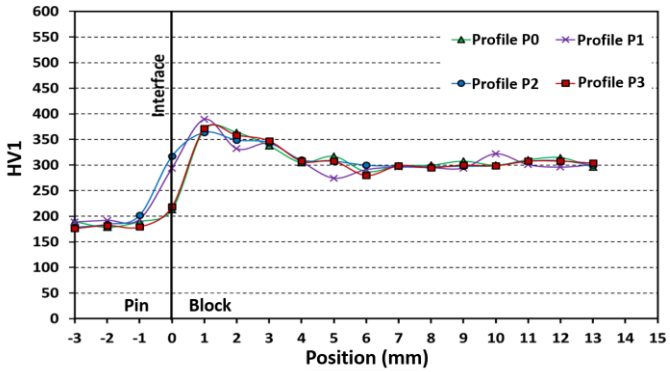

Figure 20: Sample hardness profiles (100 kN, preheating 300 °C and post heating at 600 °C).

The post-heating of 600 °C caused a considerable lowering of the hardness within the HAZ as shown in Figs. 19 and 20, with the maximum less than 400 HV.

4. CONCLUSIONS

1. The processing time is inversely related to the applied force and the test temperature;
2. The HAZ area has an inverse relationship with the applied force and direct relation with the temperature;
3. Within the Heat- Affected Zone, there is a mechanical effect at the stud/block interface simultaneously to the thermal effect, hence the region can be referred to as the Thermomechanically Affected Zone;
4. The test significantly alters the microstructure of the stud and block, mainly due to the high temperatures reached;
5. Since there was no crack formation in any of the samples, even in the untreated samples, nothing can be said about the effect of pre and post-heating on the prevention of this type of defect;
6. The 300 °C preheating caused a hardness lowering for samples processed with a force of 60 kN but not for a force of 100 kN;
7. Post-heating at 400 ^{o}C caused hardness lowering to the force of 100 kN, but not to the force of 60 kN.
8. Post-heating at 600 ^{o}C for all conditions caused reduction of the hardness to a lower and satisfactory level.

5. ACKNOWLEDGEMENTS

This work was supported by PETROBRAS

6. REFERENCES

AWS – American Welding Society, Welding Handbook, 8 ed. Miami, 1991, v 2, (0-87171-354-3).

Meyer, A., Friction Hidro Pillar Processing – Bonding Mechanismand Properties, Dissertationan der Technischen Universität Braunschweig, Hamburg, 2003.

Lebedev, V. K.; CHERNENKO, I. A. Friction Welding. Sov. Tech. Ver., 1992. v.4. p. 59 –168.

Freitas. D. S. 2014. Controle de Força e Rotação de uma Unidade de Reparo Por Atrito Usando Controlador PID e Inteligência Artificial. Dissertação de Mestrado em Engenharia Mecânica - Universidade Federal de Uberlândia, Uberlândia-MG.

Cunha, J. A. Reparo por Atrito de Elos de Corrente de Ancoragem de Plataformas Petrolíferas. 2013. Trabalho de Conclusão de Curso - Universidade Federal de Uberlândia, Faculdade de Engenharia Mecânica, Uberlândia.

Pires, R. R. Efeitos da Geometria, da Força Axial e da Rotação no Reparo por Atrito. 2007. 68 f. Dissertação de Mestrado, Faculdade de Engenharia Mecânica, Universidade Federal de Uberlândia, Uberlândia.

Dieter, G. E. Mechanical Metallurgy. 2 ed. Tokyo: McGraw-Hill Kogakusha, 1976. 774p.

Gontijo. M. F. O efeito da espessura da chapa sobre a qualidade do reparo por atrito, 2012. 112 f.. Dissertação de Mestrado - Universidade Federal de Uberlândia, Uberlândia.

7. RESPONSIBILITY NOTICE

The authors are the only responsible for the printed material included in this paper.